3D Numerical Simulation in Combustion Space of an Oxy-fuel Glass Furnace

S. X. Mei and J. L. Xie
School of Materials Science and Engineering, Wuhan University of Technology, Hubei, Wuhan 430070, China

Abstract *In glass manufacturing, oxy-fuel combustion is a new technology. In design of oxy-fuel glass furnace, the numerical simulation and virtual reality techniques have become necessary tools. In this paper, the numerical simulation in the combustion space of a designed oxy-fuel glass furnace was carried out with the results displayed by the virtual reality technology. The gas phase was expressed with k-ε two-equation model; the combustion was described with non-premixed model; the radiation was expressed with discrete ordinates radiation model. The results of simulation agree well with the related reference, showing that the flame from each burner is individual and similar, and most fuel streams combust adequately with high temperature except that from the burner 1, which is suggested to be moved to other place. What we learned from the simulation results can give direct insight in the combustion space of the furnace, and can be used to guide the design of the oxy-fuel glass furnace.*

Keywords *glass furnace; oxy-fuel; combustion space; virtual reality; numerical simulation*

1.Introduction

In glass manufacturing, the oxy-fuel furnaces, using pure oxygen instead of air as the primary oxidant, began to rapidly instead of the conventional air-fuel furnaces since 1990 because of many benefits, such as glass quality improvement, fuel reduction, productivity increase, emissions reduction (NOx, SO2, particulates), and expansion of the existing furnace [1, 2, 3]. The oxy-fuel technology is different from the air-fuel technology, to meet higher quality of the produced glass, reduce energy consumption, and prolong furnace life, it is important to obtain a rational flow field in the combustion space of the furnace. In the past，most designs of the glass furnaces were based on empirical rules or traditional methods, being difficult to obtain information such as temperatures and pressures in the combustion space of the furnace. And now with the computational fluid dynamics (CFD) modelling has been widely used to predict and estimate the flow field of the glass furnace [4, 5, 6], it is more scientific to design and optimize the oxy-fuel glass furnaces using mathematical simulation.

In this paper, an oxy-fuel glass furnace was designed, and the numerical simulation in the combustion space of the furnace was carried out. By using the virtual reality technology for the simulation results, the fields of temperature, velocity and species concentration were displayed clearly. What we learned from the simulation results can give direct "insight" in the furnace, and can be used to guide the design of the oxy-fuel glass manufacturing technology.

2.Geometrical Model

Fig. 1 shows schematically the configurations of the combustion space of the glass furnace. There are seven pairs of staggered burners, and two exhaust ports which are between the first pairs of burners. Fig. 2 shows the mesh. Structural hexahedral grid was used in the whole combustion space with mesh refined around the burners.

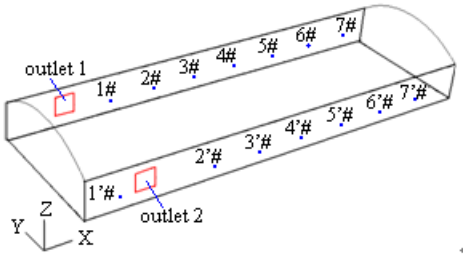

Fig.1. Configurations of the combustion space of the glass furnace

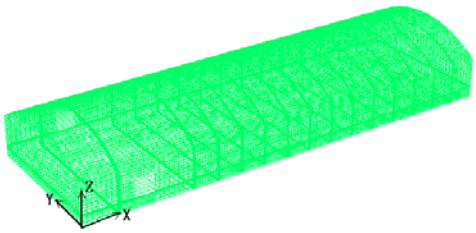

Fig.2. Meshes

3. Mathematical Model

There occur fluid flow, heat transfer, and combustion phenomena inside the combustion space. To deal with turbulence, thermal radiation, and combustion, some submodels are as follows.

3.1 Turbulence Model

In Eularian system we solve the fluid phase continuity and momentum equations using the k-ε model, which is widely used in engineering [7, 8, 9]. The general form of the governing equations for the gas phase is given as follow:

$$\partial\left(\rho v_j \varphi\right)/\partial x_j = \partial[\Gamma_\varphi \cdot (\partial\varphi/\partial x_j)]/\partial x_j + S_\varphi + S_{P,\varphi} \tag{1}$$

Where ρ is the fluid density, φ is the general different variable, Γ_φ is the effective viscosity, S_φ is the source term of the gas phase, $S_{P,\varphi}$, the sourse term from the interaction with the discrete phase.

3.2 Combustion Model

Combustion is modeled by the non-premixed modeling, which involves the solution of transport equations for one or two conserved scalars (the mixture fractions f). Equations for individual species are not solved. Instead, species concentrations are derived from the predicted mixture fraction fields. Interaction of turbulence and chemistry is accounted for with an assumed-shape Probability Density Function (PDF).

The mean (density-averaged) mixture fraction equation is:

$$\partial(\rho\overline{f})/\partial t + \nabla\cdot(\rho\vec{v}\overline{f}) = \nabla\cdot[(\mu_t/\sigma_t)\cdot\nabla\overline{f}] + S_m + S' \tag{2}$$

Where the source term S_m is due solely to transfer of mass into the gas phase from liquid fuel droplets or reacting particles (e.g., coal), and S' is any other source term.

3.3 Radiation Model

Radiation heat transfer from surface to surface and radiation absorption and emission by H_2O and CO_2 in the combustion atmosphere is modeled with the discrete ordinates (DO) radiation model [10], which solves the radiative transfer equation for a finite number of discrete solid angles, each associated with a vector direction $\vec{s}$ fixed in the global Cartesian system (*x,y,z*). The DO model transforms Equation (7) into a transport equation for radiation intensity in

the spatial coordinates (*x,y,z*). The DO model solves for as many transport equations as there are directions $\vec{s}$. The solution method is identical to that used for the fluid flow and energy equations.

$$dI(\vec{r},\vec{s})/ds+(a+\sigma_s)I(\vec{r},\vec{s})=an^2\cdot\sigma T^4/\pi+[\sigma_s\cdot\int_0^{4\pi}I(\vec{r},\vec{s}')\Phi(\vec{s},\vec{s}')d\Omega']/4\pi \quad (3)$$

Where $\vec{r}$ is the position vector, $\vec{s}$ is the direction vector, $\vec{s}'$ is the scattering direction vector, s is the path length, a is the absorption coefficient, n is the refractive index, σ_s is the scattering coefficient, σ is the Stefan-Boltzmann constant (5.672 * 10^{-8} W/m^2-K^4), I is the radiation intensity, which depends on position ($\vec{r}$) and direction ($\vec{s}$), T is the local temperature,Φis the phase function, and Ω' is the solid angle.

4. Boundary Conditions and Numerical Solution Method

The numerical procedure was based on a well-known finite volume method. To solve the elliptic form of differential equations, appropriate boundary conditions are required. (i) The fuel is natural gas with the distribution listed in Table 1, the oxidizer is pure oxy. At the inlet, all velocities and temperature were specified. (ii) At the outlet, the pressure was at an ambient atmosphere. (iii) At an impenetrable wall of the furnace, the wall temperatures on different region were specified, and the usual non-slip conditions were applied. To account for the wall effect in the nearby regions, the wall-function was introduced to link velocities in the near-wall region.

The flow field equations with boundary conditions were solved numerically. The process was repeated until convergence was achieved

Table 1 Fuel Distribution ratio (%)

No.	1#	2#	3#	4#	5#	6#	7#
distribution ratio	6	13	9.5	7.5	6	4.5	3.5
No.	1'#	2'#	3'#	4'#	5'#	6'#	7'#
distribution ratio	6	13	9.5	7.5	6	4.5	3.5

5. Results and Discussions

To visualize the flame envelope, concentration of CO (carbon monoxide) can be used as an indicator since the flame is rich in soot, which is formed in fuel-rich regions. Fig. 3 displays the iso-surface of CO concentration of 0.04. We can see the "flame" shape from each burner. Fig. 4 shows the temperature contours through the burner plane, and Fig. 5 shows the temperature contours at the vertical middle slice of burner 2.

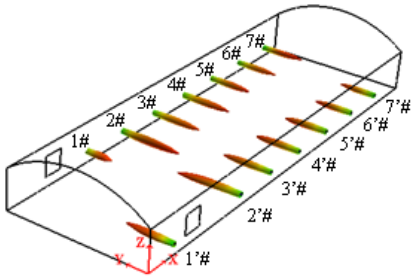

Fig.3. Iso-surface of CO concentration of 0.04

Figs. 3-5 show that not only the "flame" shape, but also the temperature field agree well with the related reference [11], indicating the reliability of the simulation results. From Figs. 3 and 4 we can see that the length and width of each "flame" from burners 2-7 correspond with the fuel

distribution ratio listed in Table 1, while the length of the "flame" from burner 1 is the shortest, indicating the incomplete combustion of the fuel.

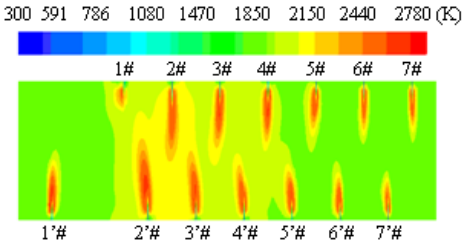

Fig.4. Temperature contours through the burner plane

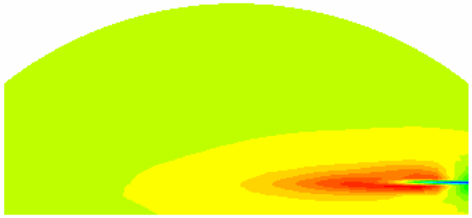

Fig.5. Temperature contour at the vertical middle slice of burner 2

Fig. 6 shows the velocity vector on the vertical middle slice of burner 2, Fig.7 displays the streamlines from burners 1-7. From Fig. 6 we can see that the gas stream runs straightly from the inlet to the opposed wall, and then rebounds when meets the wall, resulting in a wider sized reversed flows under the crown. From Fig.7 it can be observed that there is large backflow under the crown in the whole space, being beneficial for decreasing the crown heat duty.

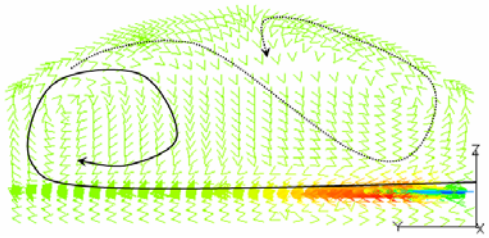

Fig.6. Velocity vector at the vertical middle slice of burner 2

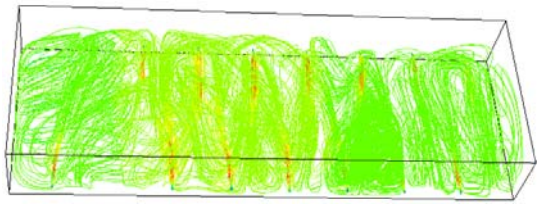

Fig.7. Streamlines from burners 1-7

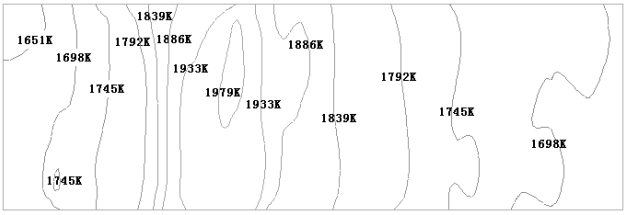

Fig.8. Temperature contours at the bottom surface

Figs. 8-10 show the temperature iso-lines at the bottom surface, the cross middle slice of burners and the crown, respectively. From Fig 9 it can be observed that the crest "flame"

temperature is around the burner 2, resulting in the corresponding local high temperature region not only on the bottom (see Fig. 8) but also on the crown (see Fig. 10). Except the high temperature region, in other regions the temperature on the bottom and on the crown is uniform.

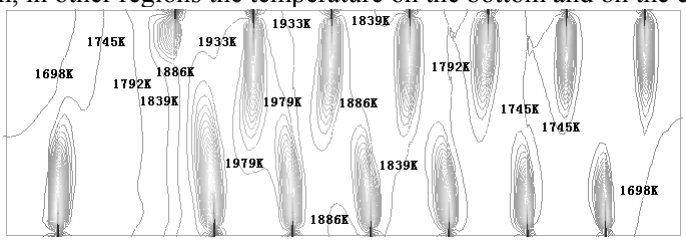

Fig.9. Temperature iso-lines at the cross middle slices of burners

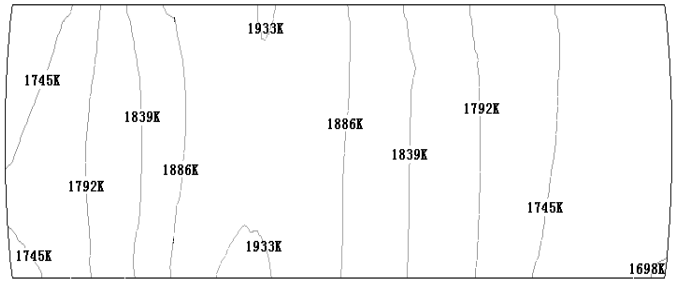

Fig.10. Temperature iso-lines at the crown

To know the temperature field along the length direction (X direction) in the whole combustion space, we created a series of vertical slices, of which the average temperature values are shown in the curve of Fig. 11. It can be observed that there are 13 temperature crests corresponding with 13 burners, except the burner 1, indicating the incomplete combustion process there, which should be improved.

The maximum of the temperature crest is near the burner 2, around which the expected hot-spot located, indicating the rationality of the results.

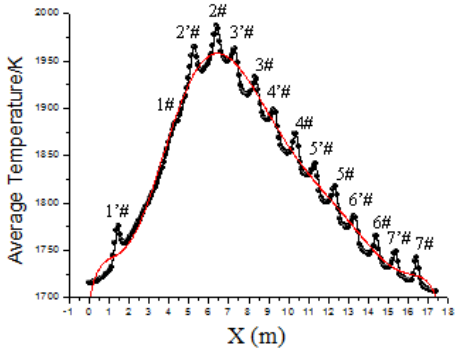

Fig.11. Average temperatures at the vertical slices along X direction

The above analyses results show that the combustion condition from the burner 1 is quite bad. It is necessary to find the reason. Fig. 12 displays the velocity vector through the burner plane, Fig. 13 shows the velocity vector at the vertical middle slice of exhaust port, and Fig. 14 displays the CO_2 concentration through the burner plane. From Figs. 12-14 it can be known that since the burner 1 is near the outlet 1, and the fuel distribution ratio of burner 1 is much less than that of the neighbor burners (2# and 2'#), when large flue gas pass by the burner 1 (see Fig. 14), and run to the outlets finally, the oxy is insufficient around the burner 1, resulting in the incomplete combustion. To improve this condition, it is suggested to move the burner 1 to other place.

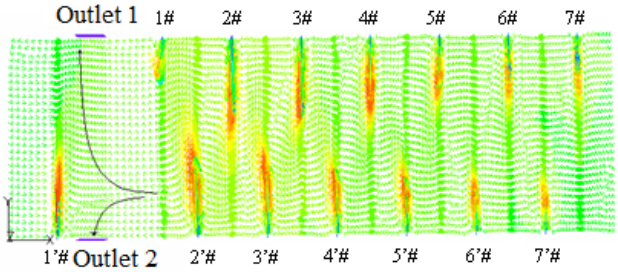

Fig.12. Velocity vector through the burner plane

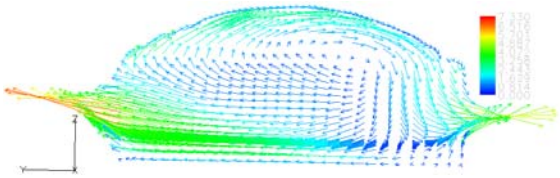

Fig.13. Velocity vector at the vertical middle slice of exhaust ports

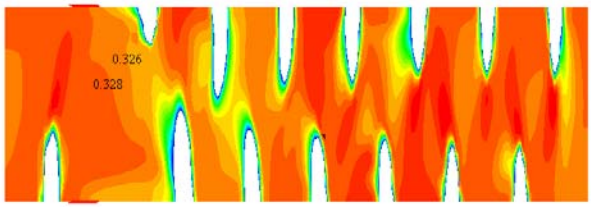

Fig.14. CO_2 concentration through the burner plane

6. Conclusion

In this paper, the numerical simulation in the combustion space of a designed oxy-fuel glass furnace was carried out. The virtual reality techniques was used to display the simulation results which are agree well with the related reference. The results show that the "flame" from each burner is individual and similar on the whole, and most fuel streams combust adequately with high temperature except that from the burner 1. The maximum flame temperature in the oxy-flames is higher than that in the air-fired furnace, and the maximum average temperature along the length direction is near the second pairs of burners, corresponding to the predicted region of hot-spot. There are back flows occurring near the crown, being beneficial for decreasing the crown heat duty. To obtain more rational flow field the placement of burner 1 will be discussed in future works.

Acknowledgements

The authors are grateful for the supports provided by the National Key Technology R&D Program (2006BAF02A26).

References

[1] Simpson, Neil G., Wilcox Richard, et al., Oxy-fuel technologies for boosting and 100% conversions of cross fired furnaces. Glass Technology: European Journal of Glass Science and Technology Part A. 48(4) (2007) 168-175.

[2] Habel Michael, Lievre Kevin, Inskip Julian, et al., Advanced Cleanfire® HRi oxy-fuel boosting application lowers emissions and reduces fuel consumption. Ceramic Engineering and Science Proceedings: 68th Conference on Glass Problems - A Collection of Papers Presented at the 68th Conference on Glass Problems. 29(1) (2008) 203-211.

[3] Kobayashi H, Evenson E., and Xue Y., Development of an advanced batch/cullet preheater for oxy-fuel fired glass furnaces. Ceramic Engineering and Science Proceedings: 68th Conference on Glass Problems - A Collection of Papers Presented at the 68th Conference on Glass Problems. 29(1) (2008) 137-148.
[4] S.L. Chang, C.Q. Zhou, and B. Golchert, Eulerian approach for multiphase flow simulation in a glass melter. Applied Thermal Engineering. 25 (2005) 3083–3103.
[5] Vishal Sardeshpande, U.N. Gaitonde, and Rangan Banerjee, Energy Conversion and Management, 48(10) (2007) 2718-2738.
[6] A. Abbassi, and Kh. Khoshmanesh, Numerical simulation and experimental analysis of an industrial glass melting furnace. Applied Thermal Engineering. 28(5-6) (2008) 450-459.
[7] U. Shah, C. Zhang, J. Zhu, et al., Validation of a numerical model for the simulation of an electrostatic powder coating process. International Journal of Multiphase Flow. 33(5) (2007) 557-573.
[8] D.M. Hargreaves, and N.G. Wright, On the use of the k–ε model in commercial CFD software to model the neutral atmospheric boundary layer. Journal of Wind Engineering and Industrial Aerodynamics. 95(5) (2007) 355-369.
[9] Fatih Üneş, Investigation of density flow in dam reservoirs using a three-dimensional mathematical model including Coriolis effect. Computers & Fluids. 37(9) (2008) 1170-1192.
[10] Jian C Q, Dutta A, Mukhopadhyay A, et al., Explicit coulpling between combustion space and glass tank simulation for complete furnace analysis. Presented at the 1st Balkan Conference on Glass Science and Technology , Volos , Greece ,2000.
[11] Lankhorst A. M., Bauer R. A., Coupled combustion modeling and glass tank modeling in oxy and air-fired glass melting furnaces. The 4th Int Sem On Mathematical Simulation in Glass Melting ,1997.